Iranian Journal of Medical Physics

ijmp.mums.ac.ir

Radiomics in IOERT of Unilateral Breast Cancer as a Biological Dosimetry

Zahra Bagherpour[1], Milad Enferadi[2], Reza Reiazi[3], Mahdie Jajroudi[4], Nahid Nafissi[5], Seied Rabi Mahdavi[1,6,*]

1. Department of Medical Physics, School of Medicine, Iran University of Medical Sciences, Tehran, Iran
2. Department of Radiology, Mayo Clinic, 4500 San Pablo Rd, Jacksonville, FL 32224, USA
3. Department of Radiation Physics, Division of Radiation Oncology, University of Texas MD Anderson Cancer Center, Houston, TX 77030, USA
4. Pharmaceutical Research Center, Mashhad University of Medical Sciences, Mashhad, Iran
5. Department of General Surgery, School of Medicine, Iran University of Medical Sciences, Tehran, Iran
6. Radiation Biology Research Center, Iran University of Medical Sciences, Tehran, Iran

ARTICLE INFO

Article type:
Original Paper

Article history:
Received: Nov 19, 2021
Accepted: Apr 06, 2022

Keywords:
Radiomics
Breast Cancer
IOERT
CT scan
Dosimetry

ABSTRACT

Introduction: In this study, Radiomic features analysis of CT scan images of the irradiated breast compared to the contralateral breast after a 12 Gy boost radiation dose in IOERT was conducted to obtain radiation-sensitive indicators (parameters) biological markers or biological dosimeters.

Material and Methods: 35 contrast chest CT scans (with unilateral ductal carcinoma in situ (DCIS) who had undergone boost IOERT) were used in this study. The total number of 259 CT radiomic features (first-order, textural, gradient, and autoregressive model-based features) were extracted using Mazda software. The features that were significantly different in the two breasts were selected. A score was assigned to each of the features and the highest scores were characterized (according to the level of significant differences). The feature selection process was performed using the hybrid feature selection method.

Results: CT Texture analysis indicated that radiation dose causes significant changes in some radiomic features of the breast tissue.

Conclusion: With more research in the future, we can fit the Delta-Radiomics values with the received radiation dose and achieve a biological dosimeter to detect low-dose radiation.

►*Please cite this article as:*
Bagherpour Z, Enferadi M, Reiazi R, Jajroudi M, Nafissi N, Rabi Mahdavi S. Radiomics in IOERT of Unilateral Breast Cancer as a Biological Dosimetry. Iran J Med Phys 2022; 19: 322-328. 10.22038/IJMP.2022.61659.2040.

Introduction

Medical imaging techniques have become one of the most essential parts of the diagnosis and medical care system due to being noninvasive in differentiating between normal and abnormal tissues, easy access, 2D and 3D assessment, and extensive role in the individualization of treatment, especially in oncology. Moreover, these images include interpretable information about tissue textures that can be quantified through mathematical algorithms to be interpreted precisely. The obtained data contain features and patterns that can be linked to different endpoints and predict them [1, 2]. The resulting features are not physically visible; however, they provide radiological textures with great quantitative information about the tissues [3–5]. The above contents define Radiomics that have been used in the medical field for only a few years. Radiomics is a new efficient post-processing method that is capable of quantifying the image's parameters. Relying on the quantitative processing of medical images (obtained from CT, MRI, PET, and other modalities), radiomics has developed appropriate algorithms to analyze hidden patterns and consider them a more accurate way to interpret images. In this field, we can determine the treatment outcome, the efficacy of the treatment, the location of the distant metastasis, and the type of tumors [6–17].

Evaluating changes resulting from treatment and medical interventions is one of the main parts of the patient's treatment process. The physician sometimes performs these assessments as a follow-up through routine tests. However, the most accurate type of evaluation is related to those evaluations that our reference is quantitative information extracted from medical images taken from the patient.

Among the most common cancers worldwide, breast cancer has the highest incidence among women worldwide [5]. The pathology, TNM, and the patient's PS (performance status) are decisive factors in determining the treatment protocol. One of the most important approaches in breast cancer treatment is surgery. In breast conservative surgery in patients with primary and local tumors, the tumor

*Corresponding Author: Email: Srmahdavi@hotmail.com; Mahdavi.sr@iums.ac.ir

bed as a possible site of later relapses (local recurrence) will be treated with complementary therapies such as radiation therapy to ensure the completion of treatment and reduce the risk of recurrence. Among all standard approaches, intraoperative radiation therapy (IORT) in both X-ray and Electron modes is one of the most recommended radiation delivery techniques in primary and local DCIS cases. Despite the radical approach, in boost intraoperative electron radiation therapy (IOERT), lower radiation dose is given to the tumor bed during surgery in the operating room which will be followed by external radiation therapy several months later [18–21].

The present work aims to evaluate the tissue changes induced by IOERT in the irradiated unilateral DCIS breast by comparing the radiomic features of the DCIS with normal breasts to determine the radiation-sensitive radiomic features.

Materials and Methods

Data acquisition

36 chest CT scans (Toshiba multi-slice 32, Japan) series of unilateral breast cancer patients diagnosed with DCIS undergoing boost intraoperative electron beam radiotherapy (12 Gy) (LIAC, Sordina, Italy) were used in the current study. To locate the exact site of the tumor bed in order to conduct treatment planning in external radiotherapy and dose delivery Surgical clips were placed in the tumor bed which improved irradiated breast tissue contouring.

ROI segmentation

We used the Mazda software [22–24] developed at the Institute of Electronics, Technical University of Lodz (TUL), Poland, by two radiologists and breast cancer surgeons (with more than 15 years of experience in this area), the contours were drawn by a radiologist. Then it was evaluated by a breast cancer surgeon and applied if it needed to be changed. In addition, the volumes of both irradiated and contralateral breasts were performed equally in each patient through a manual contouring approach (Figure 1).

Feature extraction

Following the segmentation, the radiomic features of the region of interest (ROI) were calculated. In the current study Histogram based, textural features including Gradient, Gray level run length matrix, Gray level co-occurrence matrix, and autoregressive models feature all in two-dimensional were calculated (Table 1).

Feature selection

Data were normalized between 0-1 using IBM SPSS Modeler 18.0, 2019 (IBM Inc, Armonk, New York, USA) [25]. After data normalization, analysis (including feature selection) was implemented. Feature selection assists in achieving robust features and designing powerful models for predicting different endpoints. For this purpose, we utilized the hybrid method that includes two filter and wrapper feature selection approaches [26–28].

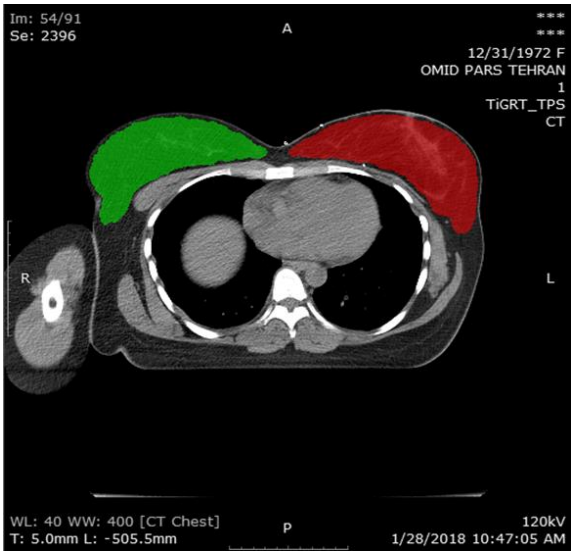

Figure 1. The ROI segmentation in CT images using Mazda software for extraction and analysis of radiomic features (red area: irradiated breast; green area: contralateral breast).

Filter method

In this method the feature selection is performed based on statistical analysis without machine learning algorithms employment [29, 30], so features are rated and weighted based on the scores they receive from Pearson's Chi-square test. This score is proportional to the (p-value) where the p-value is <0.05. The highest values of these scores indicate the highest correlation between the selected features and the point of the study (Table 2). Features with the highest score are considered input variables of the wrapper method.

Wrapper method

Wrapper selects effective features using machine-learning classifiers [26, 31, 32]. The importance of features is determined by sum-of-squares errors. In forward selection, low values of this index indicate a greater correlation between the selected feature and the target (irradiated breast). We applied three machine-learning algorithms: (1) neural network, (2) Bayesian network, and (3) Support Vector Machine (SVM). Briefly, Artificial neural networks (ANNs) generally include two fixed input and output layers and several intermediate or variable hidden layers, in addition to that, each layer contains several neurons that have a specific weight and threshold, and even though they work independently of each other, they are connected with each other. Neural networks will be able to perform effectively only if they learn accurately and have enough data. In fact, if these networks are well-trained, they will be able to classify data at a very high speed [33].

Table 1. The extracted features by Mazda software.

Row	Feature class	Feature name
1	HISTOGRAM Total number of histogram-based features: 9	Mean (histogram's mean) Variance (histogram's variance) Skewness (histogram's skewness) Kurtosis (histogram's kurtosis) Perc.01% (1% percentile) Perc.10% (10% percentile) Perc.50% (50% percentile) Perc.90% (90% percentile) Perc.99% (99% percentile)
2	GRADIENT Total number of absolute gradient-based features: 5	GrMean (absolute gradient mean) GrVariance (absolute gradient variance) GrSkewness (absolute gradient skewness) GrKurtosis (absolute gradient kurtosis) GrNonZeros (percentage of pixels with nonzero gradient)
3	RUN-LENGTH MATRIX Features are computed for 4 (2D images) Total number of run-length matrix-based features: 20 (2D) or 65 (3D)	RLNonUni (run-length nonuniformity) GLevNonU (grey level nonuniformity) LngREmph (long-run emphasis) ShrtREmp (short-run emphasis) Fraction (fraction of image in runs)
4	COOCCURRENCE MATRIX Features are computed for 5 between-pixels distances (1, 2, 3, 4, 5) Total number of co-occurrence matrix-based features: 220 (2D) or 715 (3D	AngScMom (angular second moment) Contrast (contrast) Correlate (correlation) SumOfSqs (sum of squares) InvDfMom (inverse difference moment) SumAverg (sum average) SumVarnc (sum variance) SumEntrp (sum entropy) Entropy (entropy) DifVarnc (difference variance DifEntrp (difference entropy
5	AUTOREGRESSIVE MODEL Total number of autoregressive model-based features: 5	Teta1 (parameter θ1) Teta2 (parameter θ2) Teta3 (parameter θ3) Teta4 (parameter θ4) Sigma (parameter σ)

Table 2. The statistic parameters of the final selected features.

Feature name	Min	Max	Mean	Std. dev
Teta1	-0.04	0.90	0.62	0.13
S(0 3)Correlat	-0.09	0.84	0.50	0.22
S(1 0)Correlat	0.08	0.99	0.81	0.10
Vertl_RLNonUni	699.94	8546.94	3524.18	1539.68
S(1 0)Contrast	1.373	36.502	10.87	5.57
S(1 0)DifVarnc	0.61	14.22	4.31	2.04
S(0 3)DifVarnc	1.89	48.87	14.57	7.69

Among other machine learning algorithms, we can mention the Bayesian network, where the probability of occurrence of a variable is possible based on training and data provided to the network. In fact, this algorithm determines the independent relationship of random variables. In such a way that despite the correlation of the features of a class, there is no direct connection between all the features [33].

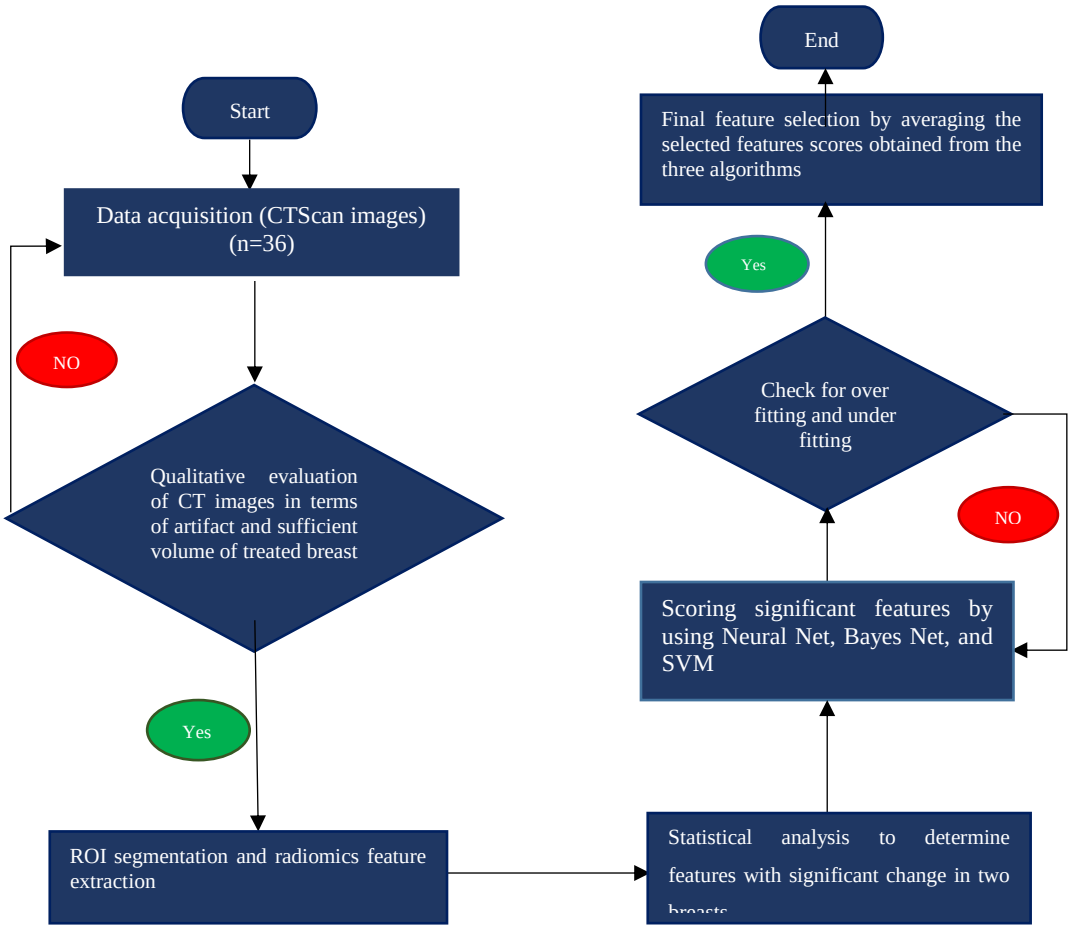

Figure 2. The workflow of images, feature extraction, and selection.

Support Vector Machine (SVM) is one of the supervised algorithms used in both classification and regression domains; however, it is mostly used in classification. Depending on the number of features of a data set (n) each data sample is drawn as a point in the n-dimensional space on the space diagram and the value of each feature related to the data is one of the components of the coordinates of the point on the diagram. In the following, a straight line will categorize different data [33].

In the end, we achieved fewer features than the filter method and a single score for each feature (by averaging the scores obtained from these three algorithms).

Figure 2 shows the workflow of our study which has been described in the following sections. It is not possible to measure the radiation dose exclusively inside the radiation field in the patient's body under treatment (although it is possible to measure the scattered dose by placing dosimeters such as film around the applicator that is not evaluated in this study). Instead, the dose reached the target volume, and the reference depth can be seen by performing previous dosimetry using phantom and calibrating the output of the device, the information obtained from TPS, and observing the Isodose curves after the treatment planning. The accelerator used in the treatment of patients under the brand name LIAC, manufactured by the Italian company Sordina in 2003, has two energy modes (10 and 12 MeV).

Results

Radiomic features

We obtained 259 radiomic features described in Table 1. Since all 259 features were not significantly different in both breasts, the number was reduced to 241 by applying the filter method. In the next step, only features that their p-value<0.05 were considered inputs for the wrapper method using Neural network, Bayesian network, and SVM algorithms. These features were assigned a score depending on the level of the feature's difference. In this study, the assessment of each algorithm was conducted separately through its receiver operating characteristic (ROC) and area under the curve (AUC) (Figure 3). The final mean of these values (for the three algorithms) was a sensitivity of 90%, a specificity of 80.3%, and the AUC of 0.9. Moreover, the Min, Max, Mean, and Standard deviation of the final features were given in Table 2. In our study,

we concluded receiving a 12 Gy dose caused structural changes in breast tissue that later appeared in radiomic features of breast tissues. These results (Teta1, S(0,3) Correlate, S(1,0) Correlate, Vertl_RLNonUni, S(1,0) Contrast, S(1,0) DifVarnc, and S(0,3) DifVarnc) can be strongly correlated with the dose of radiation (12 Gy) given to the patient in a single session (Figure 4).

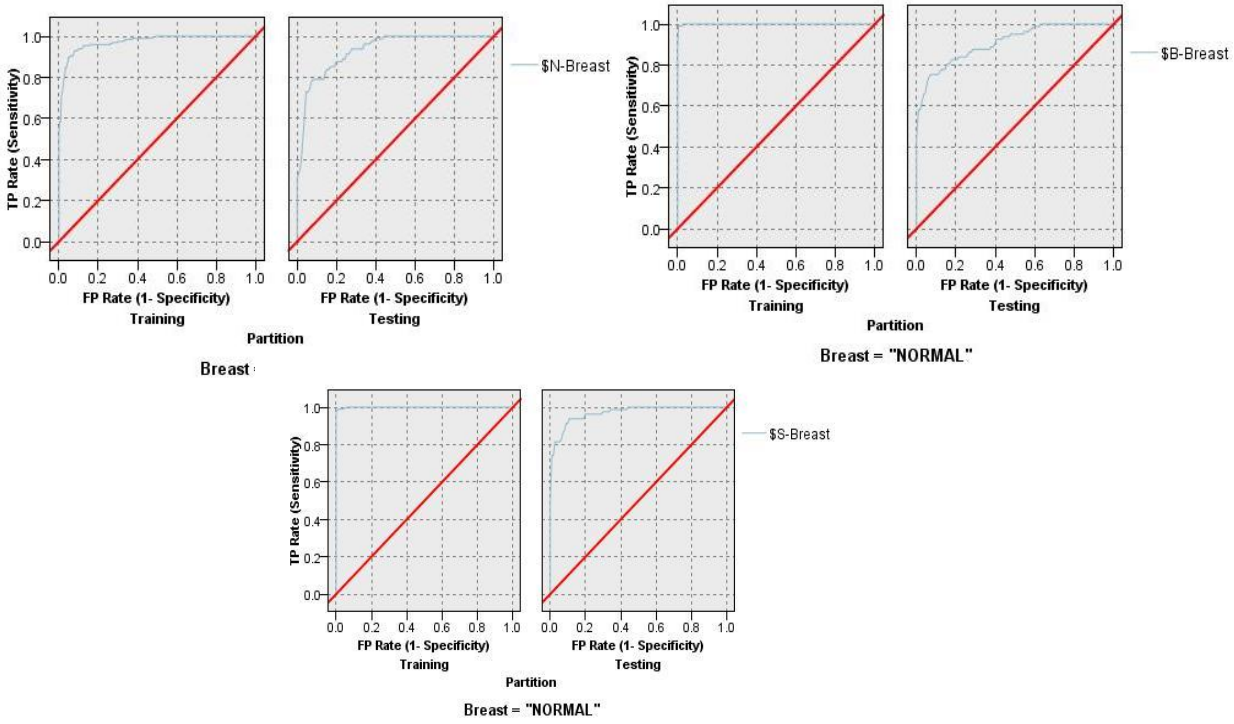

Figure 3. The receiver operating characteristic curve of each algorithm ((a) Neural network, (b) Bayes network, and (c) SVM).

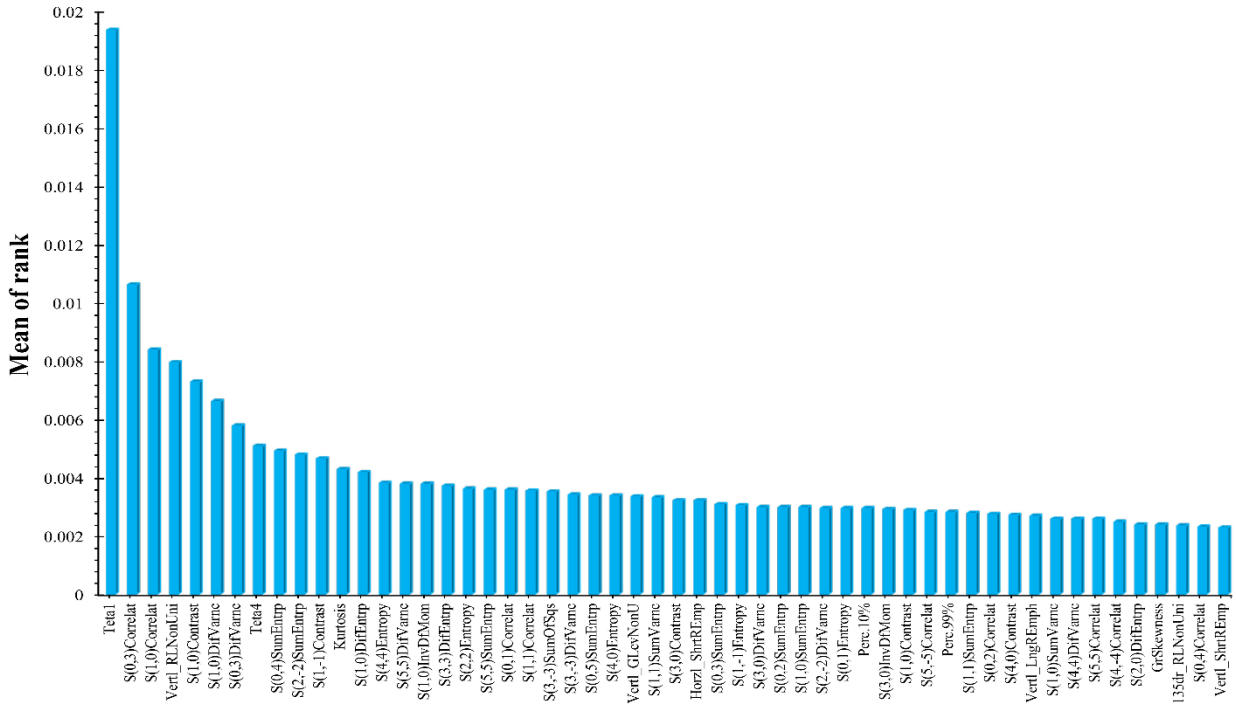

Figure 4. The selected features by the wrapper method.

Discussion

Given the particular role of all radiation therapies in cancer treatment, evaluating the consequences of receiving different radiation doses will be more important than ever, this is while the ability of radiomics in treatment evaluation, complications, and local and distant recurrences' prediction has been demonstrated. Previous studies have investigated the link between radiation dose and treatment-related complications [34–37]. Studies have shown that changes in the features after radiation are obvious. However, as we know from a radiobiological point of view, due to the complexity of the body's mechanism in damage repair, we have different effects in tissues after the fractionated dose and single dose, which requires more focused studies. In the current study, the radiomic features of the irradiated breast after mass extraction and boost IOERT and the contralateral breast were investigated, and it is concluded that some features were significantly changed. We found that there is a relationship between the radiomics features and radiation dose (12 Gy). Most of these features registered post-radiation changes, but some of them were significantly different in the two breasts, including Teta1, S(0,3Correlate, S(1,0) Correlate, Vertl_RLNonUni, S(1,0) Contrast, S(1,0) DifVarnc and S(0,3) DifVarnc had the highest differences between the two breasts. Cunliffe et al. [34] in a study evaluated radiomic features of CT scan images in patients before and after radiation therapy in order to investigate the possible relationship between esophageal radiotherapy-induced pneumonia and radiation dose and found that 12 radiomic features changed significantly after radiation therapy.

Our study aimed to investigate the ability of radiomics to detect irradiated tissue in chest CT scan images of breast cancer patients who underwent boost IOERT. According to the results, all features had different levels of variation and correlation with radiation dose. Therefore, there is a need for future studies to investigate changes in the features after receiving different doses of radiation, different time intervals after receiving radiation, and other tissues to provide a more accurate and practical correlation between the radiation dose and changes in features. Then, the use of radiomic features as a biological dosimeter in radiation dosimetry will be established.

Conclusion

The present study showed that radiation dose changes the features extracted from CT scan images of breast tissue. Further studies can be done in two general areas including model building to detect absorbed dose in breasts and other tissues and determine dedicated radiomic features to predict each complication resulting from treatment. Consequently, appropriate action can be taken to prevent or reduce the severity of the complications.

References

1. Patyk, M, Silicki, J, Mazur, R, Kręcichwost, R, Sokołowska-Dąbek, D, Zaleska-Dorobisz, U. Radiomics–the value of the numbers in present and future radiology. Polish J. Radiol. 2018;83:171–4.
2. Rizzo, S, Botta F, Raimondi S, Origgi D, Fanciullo C, Morganti AG, et al. Radiomics: the facts and the challenges of image analysis. Eur Radiol Exp. 2018;2(1):36.
3. Miles KA. How to use CT texture analysis for prognostication of non-small cell lung cancer. Cancer Imaging. 2016;16(1):10.
4. Parekh V, Jacobs MA. Radiomics: a new application from established techniques. Expert Rev. Precis. Med. Drug. Dev. 2016;1(2):207–26.
5. Valdora F, Houssami N, Rossi F, Calabrese M, Tagliafico AS. Rapid review: radiomics and breast cancer. Breast cancer research and treatment. 2018 Jun;169(2):217-29.
6. Zhao, B, Schwartz, L.H, Larson, S.M. Imaging surrogates of tumor response to therapy: anatomic and functional biomarkers. J. Nucl. Med. 2009;50(2):239–49.
7. Lambin P, Rios-Velazquez E, Leijenaar R, Carvalho S, Van Stiphout RG, Granton P, et al. Radiomics: extracting more information from medical images using advanced feature analysis. European journal of cancer. 2012 Mar 1;48(4):441-6.
8. Cook GJ, Yip C, Siddique M, Goh V, Chicklore S, Roy A, et al. Are pretreatment 18F-FDG PET tumor textural features in non–small cell lung cancer associated with response and survival after chemoradiotherapy?. Journal of nuclear medicine. 2013 Jan 1;54(1):19-26.
9. Mattonen SA, Johnson C, Palma DA, Rodrigues G, Louie AV, Senan S, et al. Radiomics versus physician assessment for the early prediction of local cancer recurrence after stereotactic radiotherapy for lung cancer. InMedical Imaging 2016: Computer-Aided Diagnosis. 2016; 9785: 359-66.
10. Larue RT, Defraene G, De Ruysscher D, Lambin P, Van Elmpt W. Quantitative radiomics studies for tissue characterization: a review of technology and methodological procedures. The British journal of radiology. 2017 Feb;90(1070):20160665.
11. Gnep K, Fargeas A, Gutiérrez-Carvajal RE, Commandeur F, Mathieu R, et al. Haralick textural features on T2-weighted MRI are associated with biochemical recurrence following radiotherapy for peripheral zone prostate cancer. Journal of Magnetic Resonance Imaging. 2017 Jan;45(1):103-17.
12. Choi W, Oh JH, Riyahi S, Liu CJ, Jiang F, Chen W, et al. Radiomics analysis of pulmonary nodules in low-dose CT for early detection of lung cancer. Medical physics. 2018 Apr;45(4):1537-49.
13. Traverso A, Wee L, Dekker A, Gillies R. Repeatability and reproducibility of radiomic features: a systematic review. Int. J. Radiat. Oncol. Biol. Phys. 2018;102(4):1143–58.

14. Vallières M, Zwanenburg A, Badic B, Le Rest CC, Visvikis D, Hatt M. Responsible radiomics research for faster clinical translation. J. Nucl. Med. 2018;59(2):189–93.
15. Bartoli M, Barat M, Dohan A, Gaujoux S, Coriat R, Hoeffel C, et al. CT and MRI of pancreatic tumors: an update in the era of radiomics. Japanese Journal of Radiology. 2020 Dec;38(12):1111-24.
16. Yang F, Ford JC, Dogan N, Padgett KR, Breto AL, Abramowitz MC, et al. Magnetic resonance imaging (MRI)-based radiomics for prostate cancer radiotherapy. Translational andrology and urology. 2018 Jun;7(3):445.
17. Jajroudi, M, Enferadi, M, Azar Homayoun, A, Reiazi, R. MRI-based machine learning for determining quantitative and qualitative characteristics affecting the survival of glioblastoma multiforme. Magn. Reson. Imaging. 2022; 85: 222–7.
18. Reitsamer R, Peintinger F, Sedlmayer F, Kopp M, Menzel C, Cimpoca W, et al. Intraoperative radiotherapy given as a boost after breast-conserving surgery in breast cancer patients. European Journal of Cancer. 2002 Aug 1;38(12):1607-10.
19. Esposito E, Anninga B, Honey I, Ross G, Rainsbury D, Laws S, et al. Is IORT ready for roll-out?. ecancermedicalscience. 2015;9.
20. Nounou MI, ElAmrawy F, Ahmed N, Abdelraouf K, Goda S, Syed-Sha-Qhattal H. Breast cancer: conventional diagnosis and treatment modalities and recent patents and technologies. Breast cancer: basic and clinical research. 2015 Jan;9:BCBCR-S29420.
21. Lei J, Wang Y, Bi Z, Xue S, Ou B, Liu K. Intraoperative radiotherapy (IORT) versus whole-breast external beam radiotherapy (EBRT) in early stage breast cancer: results from SEER database. Japanese Journal of Radiology. 2020 Jan;38(1):85-92.
22. Szczypinski, P, Strzelecki, M, Materka, A. MaZda - a Software for Texture Analysis. Proc. of ISITC. 2007:245–9.
23. Szczypinski P, Strzelecki M, Materka A, Klepaczko A. MaZda-A software package for image texture analysis. Comput. Meth. Prog. Bio. 2009;94(1):66–76.
24. Strzelecki M, Szczypinski P, Materka A, Klepaczko A. A software tool for automatic classification and segmentation of 2D/3D medical images. Nuclear Instruments and Methods in Physics Research Section A: Accelerators, Spectrometers, Detectors and Associated Equipment. 2013 Feb 21;702:137-40.
25. IBM Corp., IBM SPSS Modeler 18.0, https://www.ibm.com/support/pages/downloading-ibm-spss-modeler-180, 2019, Armonk, NY, USA.
26. Hsu HH, Hsieh CW, Lu MD. Hybrid feature selection by combining filters and wrappers. Expert Systems with Applications. 2011 Jul 1;38(7):8144-50.
27. Cadenas JM, Garrido MC, MartíNez R. Feature subset selection filter–wrapper based on low-quality data. Expert Syst. Appl. 2013;40(16):6241–52.
28. Hu, Z, Bao, Y, Xiong, T, Chiong, R. Hybrid filter–wrapper feature selection for short-term load forecasting. Eng. Appl. Artif. Intell. 2015;40:17–27.
29. Sakai K, Yamada K. Machine learning studies on major brain diseases: 5-year trends of 2014–2018. Jpn J Radiol. 2019;37:34–72.
30. Alis D, Bagcilar O, Senli YD, Yergin M, Isler C, Kocer N, et al. Machine learning-based quantitative texture analysis of conventional MRI combined with ADC maps for assessment of IDH1 mutation in high-grade gliomas. Japanese Journal of Radiology. 2020 Feb;38(2):135-43.
31. Das S. Filters, wrappers, and a boosting-based hybrid for feature selection. ICML '01: Proceedings of the Eighteenth International Conference on Machine Learning. 2001;74–81.
32. Jantawan B, Tsai CF. A comparison of filter and wrapper approaches with data mining techniques for categorical variables selection. International Journal of Innovative Research in Computer and Communication Engineering. 2014;2(6):4501-8.
33. Uddin S, Khan A, Hossain ME, Moni MA. Comparing different supervised machine learning algorithms for disease prediction. BMC Med Inform Decis Mak. 2019;19(1):281. Doi:10.1186/s12911-019-1004-8
34. Cunliffe A, Armato III SG, Castillo R, Pham N, Guerrero T, Al-Hallaq HA. Lung texture in serial thoracic computed tomography scans: correlation of radiomics-based features with radiation therapy dose and radiation pneumonitis development. International Journal of Radiation Oncology* Biology* Physics. 2015 Apr 1;91(5):1048-56.
35. Moran A, Daly ME, Yip SS, Yamamoto T. Radiomics-based assessment of radiation-induced lung injury after stereotactic body radiotherapy. Clinical lung cancer. 2017 Nov 1;18(6):e425-31.
36. Abdollahi H, Mahdavi SR, Shiri I, Mofid B, Bakhshandeh M, Rahmani K. Magnetic resonance imaging radiomic feature analysis of radiation-induced femoral head changes in prostate cancer radiotherapy. Journal of cancer research and therapeutics. 2019;15(8):S11-9.
37. Abdollahi H, Tanha K, Mofid B, Razzaghdoust A, Saadipoor A, Khalafi L, et al. MRI radiomic analysis of IMRT-induced bladder wall changes in prostate cancer patients: a relationship with radiation dose and toxicity. Journal of Medical Imaging and Radiation Sciences. 2019 Jun 1;50(2):252-60.